FACTA UNIVERSITATIS (NIŠ)
SER.: ELEC. ENERG. vol. 23, no. 1, April 2010, 1-16

The Application of Computational Electromagnetics to Microwave Dielectric Gauging

Invited paper

Nathan Ida

Abstract: Gauging of dielectrics – the accurate evaluation of material properties and geometrical dimensional measurement are discussed first, followed by application of computational electromagnetic methods including FEM, FDTD and TLM for the simulation and evaluation of properties as well as for the design of devices and testing configurations. Microwave microscopy is used for testing in dielectrics in an open antenna configuration. This is followed by modelling and application of closed and open resonant structures for material properties determination and finally an open resonant structure for accurate determination of rubber thickness in an industrial sensor is described. The use computational electromagnetic tools is seen as indispensable for the design of these testing geometries.

Keywords: Resonant structures, numerical methods, computational electromagnetics, nondestructive testing.

1 Introduction

GAUGING is defined in different ways, depending on the area of application. In this work we use a general definition, that of accurate measurement of a property or dimension. The problem of gauging in dielectrics therefore, has two different aspects. One is the issue of accurate measurement of material properties permeability, permittivity and conductivity. The second, equally important is that of accurate measurement of dimensions such as thickness. These two distinct areas of measurement are important in design and testing and have important applications

Manuscript received on November 19, 2009. An earier version of this paper was presented at 9th International Conference on Applied Electromagnetics August 31 September 02, 2009, Niš, Serbia.

The author is with The University of Akron, Department of Electrical and Computer Engineering, Akron, Ohio, 44325-3903, USA (e-mail ida@uakron.edu).

such as monitoring of production of dielectrics or in the curing processes of dielectrics such as rubber. Additional applications are in monitoring of pollutants and solvents either for safety or health purposes. In all of these applications the accurate measurement of a property is critical for the functioning of a system or for detection of a property related to functionality. Gauging can take many forms including electrostatic (capacitive measurements), optical (laser microscopy), acoustic (time of flight measurements for dimensional gauging) and others but we will discuss here only methods associated with microwaves. Specifically, we will discuss microwave resonant methods including microwave microscopy for the purpose of dimensional gauging and for material properties evaluation. Although microwave measurements, and in particular dimensional measurements are not usually considered accurate enough because of the relatively long wavelength, it is possible to conduct dimensional measurements down to the micrometer scale and material properties variations so small that the term microwave microscopy is appropriate. In particular, resonant methods, coupled with network analyzers can be used to detect the slightest variation in properties and thus the method becomes a useful tool in testing and evaluation. Coupled with this is the challenge of computation of the test configuration for design and optimization purposes. The use of computational electromagnetics methods are uniquely qualified to simulate and, indeed, analyze testing geometries for gauging purposes because they can accurately model both geometrical and material properties. The use of numerical methods simplifies the task of design of testing configurations and can generate useful calibration profiles for material properties and their variations.

Three numerical methods will be discussed here in conjunction with their use for gauging purposes. The FDTD method is used in conjunction with prediction of resonant frequencies in open resonators used for testing and monitoring of rubber products in industrial production. The Transmission Line Method (TLM) is used for modeling of microwave microscopy in open geometries, for nondestructive testing of dielectrics whereas the Finite Element Method (FEM) is shown to be useful in predicting resonant frequency and their shift due to loading of closed and open cavities. There are many other methods and variations that have been used for these purposes but we will concentrate on the three methods above for brevity and because they represent classes of computational methods. Some examples of the use of these numerical methods are also given.

2 Microwave Microscopy

Microwave scanning microscopy is an important method in nondestructive testing and evaluation of materials. It can be applied to all materials but is particularly use-

ful in dielectrics. Because of this, it has been applied in a variety of areas including micro-crack detection in aircraft, biological investigations, in the semiconductor industry and in civil engineering. Microwave propagation is affected by a large number of material properties including composition, structure, moisture, discontinuities, density variations and, of course permeability and permittivity. Hence the value of a good mathematical model of the testing geometry is imperative [1]. Very high resolution can be achieved with probes that can work in-situ and on line. In the microwave frequency region, variation of dielectric permitivity for dielectric materials is significantly larger than the contrast due to density. The physical application of microwave microscopy consists of an antenna configured as an open resonator connected to a network analyzer. The antenna can be as simple as an open ended coaxial cable with the inner conductor extending beyond the outer conductor to form a resonant antenna. This probe or sensor is then scanned over the medium in which it is to detect cracks or material properties variations. Typically, it is in very close proximity with the medium (typically a few micrometer) and detection is affected by scanning the probe over the medium in very small steps over relatively small areas. As such, the method can be considered a "near field" method. Most numerical methods cannot handle this type of configuration successfully and, in particular, formulations that allow for computation of resonant frequencies as well as quality factors in open or close cavities such as the finite element method fail in this case because of the minute dimensions involved and the need to model extensive areas (the antenna length, for example is of the order of 1-5 cm, whereas cracks in dielectrics may be of the order of a μm).

The Transmission Line Matrix (TLM) method is a time domain technique that can deal with complex geometries and is particularly suited to model microwave testing of the type described above. Although the method has other advantages, including the ability to model intricate geometries, the main attraction of the method is that it can be considered to be "a modeling process rather than a numerical method for solving differential equations" [2]. The TLM provides direct simulation of the phenomenon and not of the equation governing it [3]. This means that a signal can be propagated throughout the computational domain and the resulting interaction of the signals and geometry at every step can be monitored to follow the physical process involved. At its basis the method consists of dividing a geometry into a set of nodes on a grid which can be arbitrary but more of ten are regularly distributed. The nodes are connected with transmission line sections whose properties reflect the medium between the nodes. The grid so obtained may be viewed as a structure of transmission line sections in which the signals propagate along the transmission line sections and reflect and transmit at nodes where sections meet. The voltages at nodes are then calculated based on the propagation properties of the sections and the reflection and transmission coefficients at

the nodes. The method used here is based on the symmetrically condensed node (SCN) [4]. The SCN is ~~a node with the~~ 6 transmission line sections emanating from a node (the center of the cell) that connect to the grid. The connections to the grid are in mid-section between nodes. The voltages at the interfaces with the grid are calculated using a scattering matrix. The scattering matrix implementation of SCN is based on calculation of voltages on the grid. Assuming a rectangular grid (i,j,k), the reflected voltages at any port are obtained using the following Vscheme [5]:

$$V^r_{inf} = \frac{1}{2}(V_{kni} + V_{kpi} + V_{dif} - V_{ipj} + V_{inj}) \tag{1}$$

$$V^r_{ipj} = \frac{1}{2}(V_{kni} + V_{kpi} + V_{dif}) \tag{2}$$

where n, p, indicate negative and positive directions of propagation, r indicates reflected components.

The S_{11} parameter is used to obtain a microwave image. This parameter ~~can not~~ be obtained directly from the TLM algorithm because an incident field ~~can not~~ be separated from the total field. To solve this problem two successive runs of the program are needed. The first run is performed with excitation without a reflecting object. This run will provide data for the reference port. A second run of the program will be performed considering boundary conditions for objects to be investigated. The S_{11} parameter is given by:

$$S_{11} = \frac{F_i - F_0}{F_i + F_0} \tag{3}$$

In (3), F_0 and F_i are the frequency responses obtained for the same position of excitation source without reflecting object and with reflector respectively.

Fig. 1 shows the plot of the S11 parameter for metal, bakelite ($\varepsilon_r = 5$) and teflon ($\varepsilon_r = 2$). The plot demonstrates the capability of the proposed TLM model to differentiate between the materials with different electric permitivities. The frequency response was obtained after two intermediary signal processing steps: filtering and windowing. The same signal processing process was applied to the reference and reflected signals.

Fig. 2 shows the numerical results for simulation of scanning over two small pieces of bakelite and teflon respectively. The length of dielectric pieces was 1.6 mm and step size in scanning was 0.033mm. The dielectric profiles were obtained by selecting the corresponding computed S11 for 1.72GHz. This procedure is identical to that used in experimental microwave microscopy [6].

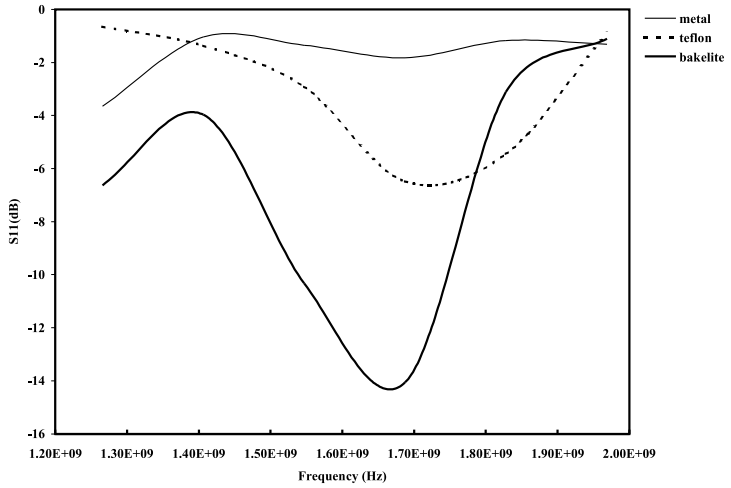

Fig. 1. The S_{11} parameter extracted from the TLM generated signals for different materials.

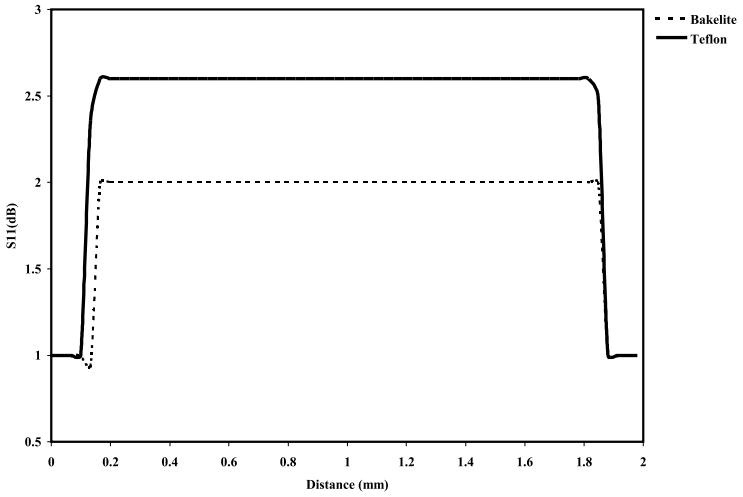

Fig. 2. Results of numerical scanning for two pieces of dielectric.

3 Testing and Monitoring in Resonant Structures

In addition to the open structure of a resonant antenna, there are a number of other basic resonant methods that are suitable for testing [1, 7]. Resonant methods rely on the shift in resonant frequency of an open or closed resonant cavity or resonant

transmission line due to variations in material properties. The fundamental structure is that of a closed cavity in which the test medium resides. This is typical of testing an monitoring of gases, fluids, and samples of solid objects that either fill the cavity or only occupy a small part of the volume. The method can be easily adapted for continuous testing and monitoring of materials. Fig. 3a shows a continuous material such as a tubular dielectric or a fluid passing though a cylindrical cavity resonator. Fig. 4b shows a cavity resonator with a flat material passing

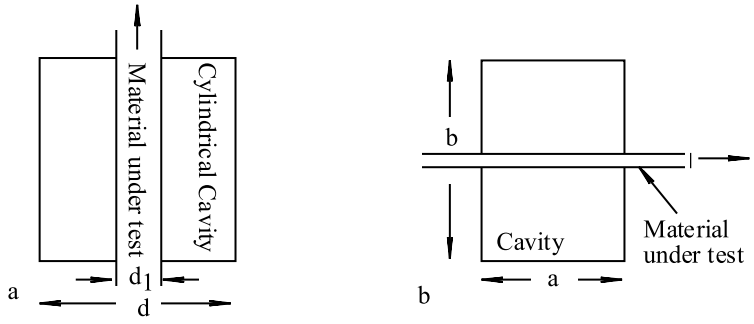

Fig. 3. Continuous monitoring in microwave cavities.

through the cavity. The cavity may in fact be made as two half "boxes" of cylindrical or rectangular shape, placed on two sides of the test sample. A third basic method is shown in Fig. 4. Here the test sample is outside the cavity resonator. Fig. 4 shows an aperture coupled cavity test. The basic principle here is that the

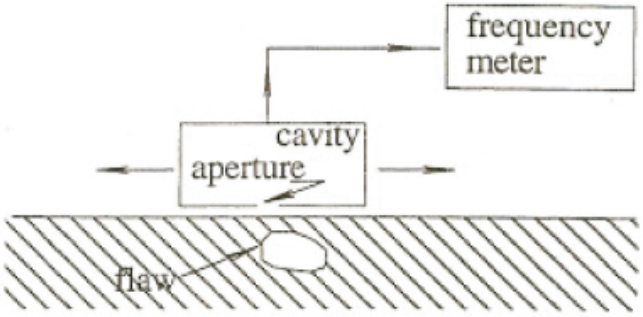

Fig. 4. Testing with open cavities.

external material influences the conditions in the cavity but, because the cavity is open, it is often easier to perform the required tests. In particular, Fig 4 is in fact a variation of the microwave microscopy method described above where the aperture

has replaced the antenna. In all methods, the resonant frequency and/or the quality factor of the cavity are monitored to indicate the effects of the materials.

4 Models for Resonant Cavities

There are a number of possible models for computation in resonant structures. Three general models are discussed here. These are the eigenvalue model, the deterministic model and the aperture model. The models inhomogeneities in materials, and can also model the coupling between waveguides and cavities so that the effect of sources can also be modeled. Lossy and lossless dielectrics can be treated equally well. The sensing parameter is the cavity's resonant frequency although other parameters such as the Q factor or, for that matter, fields within the cavity, standing wave ratios in the waveguide and the like may be obtained. These are described briefly next.

4.1 The Eigenvalue model

In this model, the eigenvalues (corresponding to the resonant frequencies of the cavity) are computed. The formulation of a finite element model starts with the field equations. In this case this is the source free Helmholtz equation:

$$\nabla \times (\frac{1}{\mu_r} \nabla \times \boldsymbol{E}) = k_0^2 \varepsilon_r \boldsymbol{E} \tag{4}$$

where $k_0^2 = \omega^2 \mu_0 \varepsilon_0$, ω is the angular resonant frequency, μ_0 and ε_0 are the permeability and permittivity of free space and μ_2 and ε_r are the relative permeability and permittivity of materials. Eq. (4) describes a characteristic value problem, that is, for each characteristic value k_0 it has a solution for $\boldsymbol{E}$: To solve this problem using finite elements, we first use an equivalent functional of Eq. (4) obtained through a variational approach:

$$f(\boldsymbol{E}) = \frac{1}{2} \int_v \left[\frac{1}{\mu_r} (\nabla \times \boldsymbol{E}) \cdot (\nabla \times \boldsymbol{E}) - k_0^2 \varepsilon_4 \boldsymbol{E} \boldsymbol{E} \right] \mathrm{d}v \tag{5}$$

where v is any volume of interest. To discretize the domain we use edge finite elements which allow a discontinuity in the normal component of the field but enforce continuity of the tangential component [8]. For any finite element, the approximation for the electric field is:

$$\boldsymbol{E} = \sum_{i=1}^{n} E_i \boldsymbol{w}_i \tag{6}$$

where n is the number of unknowns on the edges and E_i are the unknown values of the tangential electric field intensity along the edges of the finite element. Substitution of this approximation in (5) and application of the Ritz procedure gives the following matrix system:

$$[A][E] = k_0^2[B][E] \tag{7}$$

where the coefficients of matrix $[A]$ and $[B]$ are:

$$\begin{aligned} a_{mn} &= \int_{v_i} \Big[\frac{1}{\mu_r}(\nabla \times \boldsymbol{w}_m) \cdot (\nabla \times \boldsymbol{w}_n)\Big] \mathrm{d}v \\ b_{mn} &= \int_{v_i} \varepsilon_r [\boldsymbol{w}_n \cdot \boldsymbol{w}_n] \mathrm{d}v \end{aligned} \tag{8}$$

and v_i is the volume of the ith element. Eq. (7) can be solved as an eigenvalue problem for the values of k0 (eigenvalues) and the field vector $\boldsymbol{E}$ (eigenvectors), provided that the correct boundary values are applied. From the electric field intensity vector and the resonant frequency, other parameters such as energy may be evaluated.

4.2 The deterministic model

The deterministic model does not require the calculation of eigenvalues but only of fields. In effect, an eddy current formulation, based on the magnetic vector potential [1], is modified to allow the computation of electromagnetic fields at high frequencies such as waveguides and cavities by adding the coupling between the electric and magnetic fields. This type of formulation is particularly attractive for NDT applications since it allows calculation of conduction as well as dielectric losses and is applicable to a wide range of practical geometries. The effect of displacement currents can be added by including the electric field directly in the formulation. A general formulation that includes displacement currents is:

$$\frac{1}{\mu}\nabla^2 \boldsymbol{A} = \boldsymbol{J}_s - \omega^2 \varepsilon \boldsymbol{A} - \sigma(j\omega \boldsymbol{A} + \nabla\psi) \tag{9}$$

where ψ is the electric scalar potential. If significant eddy currents exist, (as in the case of high loss materials), the eddy currents must also be constrained in the solution domain to ensure uniqueness of the solution. The continuity equation is used for this purpose [1]:

$$\nabla \cdot (j\omega\sigma \boldsymbol{A} + \sigma\nabla\psi) = 0 \tag{10}$$

The only assumption implicit here is the use of Coulombs gauge. After the magnetic vector potential is calculated, either $\boldsymbol{B}$ or $\boldsymbol{E}$ can be calculated. The magnetic flux density is calculated from $\boldsymbol{B} = \nabla \times \boldsymbol{A}$ and the electric field intensity from $\boldsymbol{E} = -(j\omega \boldsymbol{A} + \nabla\psi$.

The solution to Eqs. (9-10) leads to the correct field quantities based on the general field representation at any frequency. This is a deterministic approach where the source is assumed to be known. For this reason the modes of a cavity cannot be obtained directly. However, the method is not restricted to cavities or to high frequency problems. For any given frequency, a solution is obtained. By scanning a frequency range (i.e. solving a number of eddy current problems, each at a different frequency), the resonant frequencies can be detected. For the purpose of detecting resonance or shift in resonant frequency, the total stored energy in the cavity is calculated. A peak in the stored energy indicates resonance. This choice is convenient in that the actual energy in the system is not important, only the relative values. For a cavity, the actual fields are difficult to calculate because Eq. (9) requires the actual source distribution. This means that the sources and their coupling to the cavity must be modeled accurately. If only relative terms are required, an arbitrary source can be used as long as the source supports the mode (or modes) required. From these relative energy terms, the resonant frequency and the Q-factor can be calculated. If the fields themselves are needed, the source, and the coupling to the cavity must be modeled.

4.3 The Aperture model

This model is an outgrowth of a more general scattering model which goes beyond resonant structures but it is representative of a class of models that can take into account open structures as well as closed structures. We start with Eq. (4) but rewrite it as:

$$\nabla \times (\frac{1}{j\omega\mu}\nabla \times \boldsymbol{E}) - J\omega\varepsilon\boldsymbol{E} = 0 \tag{11}$$

To formulate this equation in terms of finite elements, approximations identical to those in Eq. (6) are used for the electric field. Doing so for the electric field, using the Galerkin method with weighting functions wm and integrating over the volume gives:

$$\int_v (\frac{1}{j\omega\mu}\nabla \times \boldsymbol{E}) \cdot (\nabla \times \boldsymbol{w}_m)\mathrm{d}v + \int_v j\omega\varepsilon\boldsymbol{E} \cdot \boldsymbol{w}_m \,\mathrm{d}v = \int_S (\hat{\boldsymbol{n}} \times \boldsymbol{H}) \cdot \boldsymbol{w}_m \mathrm{d}s \tag{12}$$

This is a coupled volume-surface integral equation. Its solution is best handled by boundary elements on the boundary of the cavity or open resonator while the interior is modeled as a finite element problem. In particular, the equivalent surface current density in the aperture can be evaluated to obtain the effect of external materials on the resonant frequency of the cavity.

The eigenvalue formulation in the previous section was applied to the problem shown in Fig. 5. It consists of a cylindrical cavity coupled to a rectangular waveguide through an iris of varying dimensions. A cylindrical dielectric test sample is

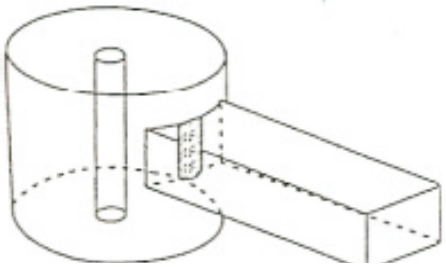

Fig. 5. Geometry of a cavity and waveguide section.

placed at the center of the cavity to simulate a particular test such as the one in Figure 2a. The cavity is excited through the rectangular iris from the waveguide which operates in the TE_{10} mode. The dominant resonant mode in the cavity is the TE_{101} mode and equals 2.594 GHz for the empty cavity. To generate the waves in the waveguide, a Dirichlet boundary condition $E_y = \sin(\pi x/a)$ is applied on the cut on the waveguide which is chosen as one wavelength long at the empty cavity resonant frequency. To see how the resonant frequencies change with the presence of different materials, a 7 or 9 mm Plexiglass rod ($\varepsilon_r = 2.7 + j0.01$), a 7 or 9 mm PVC rod ($\varepsilon_r = 4 + j0.05$) or empty cavity are analyzed for different coupling iris sizes. The results, obtained using the formulation in (4) through (11) are shown in Fig. 6. They show first that the change in resonant frequency is quite significant for any of these materials while the size of the iris matters little.

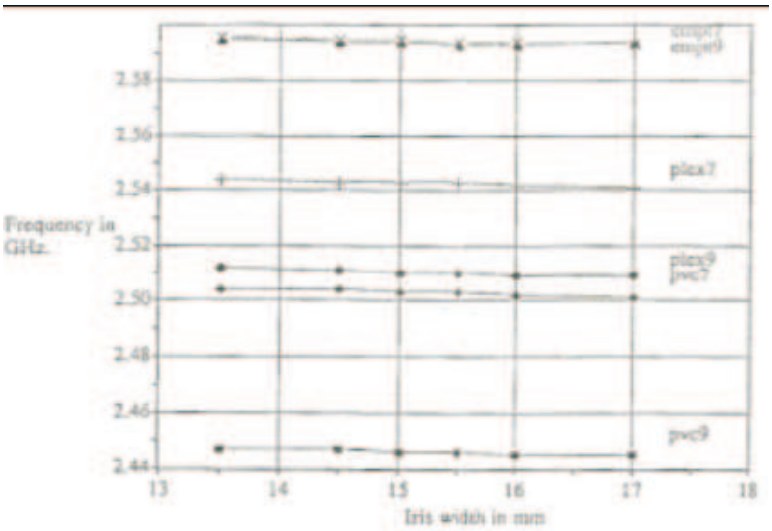

Fig. 6. Resonant frequency versus iris width for different loadings.

5 An Open Stripline Resonator for Microwave Gauging

Previous work with open resonators has shown that a variety of dielectric media can be accurately tested and measurements for a variety of parameters is possible [9–11]. It has been used in the past for a number of applications including monitoring of paper thickness and drying [12], moisture monitoring in wood [13], and even in monitoring the drying of grain [14]. More recently, we have shown that an open resonators in combination with a network analyzer can be used in the industrial environment for measurement of rubber products in real time and for the purpose of product improvement [15].

The sensor described here is different than previous sensors. First, the present sensor operates against a conducting surface on which the dielectric moves. The sensor is curved to conform with the conducting cylinder. Second, the sensitivity is much higher, primarily due to the use of the network analyzer but also from the design of the cavity and the motion system. Third, a complete analysis and simulation of the system has been carried out allowing for diverse influences including effects of moisture, temperature, contamination, proximity of personnel and many others as well as optimization of the sensor components themselves - stripline plates dimensions, shape spacing and location, coupling probes, shielding structure and others. In addition, the system incorporates automatic on-line calibration through use of reference sheets that bound the expected permittivity of the production material above and below, thus ensuring correct measurement of permittivity while removing uncertainties associated with environmental conditions.

5.1 Sensor Design

The design of the sensor system started with a double center-conductor stripline resonator shown in Fig. 7. A resonator of this type is expected to have two modes: an odd mode and an even mode [7, 8]. The figure also shows possible coupling probes. This configuration is also known as broadside coupled stripline. The two resonant modes are defined by the capacitances of the empty cavity, the inductance and, of course, the permittivity of the measured fabric. The resonant frequencies of the cavities when the sample is present are given by:

$$f_o = \frac{1}{2\pi\sqrt{\mu_0 \dfrac{c_o}{c_{o0}}}}, \quad f_e = \frac{1}{2\pi\sqrt{\mu_0 \dfrac{c_e}{c_{e0}}}} \tag{13}$$

where c_o and c_e are the capacitances for the odd and even mode and c_{o0} and c_{e0} are the capacitances for the even/odd modes when the cavity is empty [8]. In the sensor described here these relations are only approximate since Eq. (13) assumes

a uniform transmission line, whereas in our case the stripline only extends part of the length of the cavity.

In the even mode, the fields are parallel to the surface of the dielectric whereas in the odd mode they are perpendicular [16]. Because of the fact that the fabric is thin and, hence the total perturbation volume in the cavity is small, the dielectric will influence the frequency of the odd mode very little the shift in the odd resonant frequency due to the presence of the fabric is proportional to $(\varepsilon_r - 1)/\varepsilon_r$ with er the relative permittivity of the fabric (assuming the perturbation is small). In the even mode, with the electric field parallel to the dielectric, the shift in resonant frequency is proportional to $(\varepsilon_r - 1)$ [17]. Clearly the shift in resonant frequency of the even mode is much higher. Also, it should be noted that the odd and even mode frequencies are different with the even mode resonant frequency being lower. The use of the even mode frequency, although sensitive to both changes in permittivity (moisture content) and thickness of the dielectric, imposes some restrictions on the measurements. The most serious of these is the need to keep the sample at a fixed relative position with respect to the resonator plates, preferably at the exact center. In particular, vertical motion of the sample will result in errors in measurements. This restriction is not as serious with the odd mode since the fields around the center of the cavity tend to be more uniform. For this reason, the odd-mode resonant frequency has been suggested as a means of compensating for common-mode effects such as humidity and temperature [9, 11].

The two probes shown are used as a source and load probe for the network analyzer to monitor the S parameters. The excitation is through the gap between the probe and upper plate. To detect resonance only the S11 parameter is needed since at resonance the S11 parameter exhibits a sharp drop. The sensor just described has been used previously to monitor thickness and water content in a latex coated fabric production line [15]. In that application, the fabric moved along the center plane between the two plates.

In the production of rubber sheets, the rubber passes over a cylindrical drum called calendar which both maintains its thickness and keeps it flat. For this purpose it was deemed essential that the rubber thickness be measured while the rubber sheet moves across the calendar. To do so, the sensor of Fig. 1 was modified in two ways. First, only the upper section was used complete with the two probes. Second, the sensor was made conformal by changing the plates and the shield to curved structure so that the distance between calendar and sensor components is constant. The sensor is shown schematically in Fig. 2. It is quite different than the structure in Fig, 7 but, as can be verified through application of image theory, the fields of the two structures are very similar, the main differences being introduced by the curvature of the structure in Fig. 2. In addition, the introduction of the conducting surfaces is expected to change the modes since the odd mode fields,

which are expected to be parallel to the surface must necessarily be suppressed by this configuration. The even mode on the other hand should change very little. The basic dimensions were left the same. The sensor is 50 cm long, 30 cm wide and 7 cm thick (the sensor in Fig. 8 is shown in cross section across its width the second probe is behind the one shown). To optimize the sensitivity of the new sensor, the first adjustment was to make the geometry itself conformal by bending all conductors so that the distance between conductors and calendar is the same everywhere. This change further changes the resonant frequencies but also allows for more uniform coverage of the dielectric surface. A relatively low resonant frequency around 400 MHz was used based on previous experience with this type of resonators, a frequency dominated primarily by the dimensions of the cavity [15].

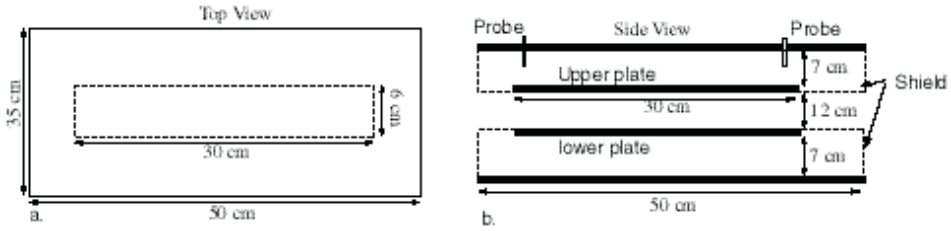

Fig. 7. Structure and dimensions of a simple open resonant sensor. The shield is made of two open boxes that also serve as the ground planes.

To cover the entire width of the rubber sheet (150 cm) the sensor moves across the fabric back and forth. Calibration sheets are placed on either side of the fabric and calibration is achieved by simply extending the motion of the sensors. The motion is achieved by a screw driveor a belt. The whole system is controlled through a computer which also schedules the calibration steps, acquires and stores the data and communicates to the control center.

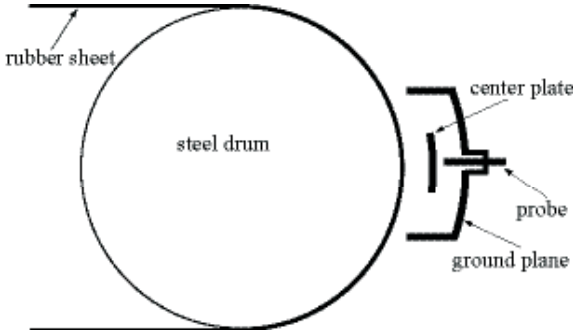

Fig. 8. The curved resonant sensor in position next to the rubber sheet. The steel drum is 76cm in diameter and the sensor is spaced 3.5 cm from the drum.

The simulations were carried out using FDTD, first using a general purpose program followed by a commercial program. The purpose of simulations was to define the limiting parameters of the system including expected sensitivity, and optimization of the various parameters including dimensions prior to construction. Fig. 9 shows the first two resonant frequencies (both even mode) as obtained with the structure in Fig. 8. The rubber is 1mm thick and the sensor is separated 3.5 cm from the drum. The first resonant frequency occurs at 419.8 GHz, the second at 824.8 GHz. Simulations were carried out at both frequencies but in the implementation only the first frequency was actually used.

The most important issue in the design was the sensitivity of the sensor to rubber thickness. Fig. 10 shows the sensitivity to rubber thickness at various sensor spacings between the sensor at steel drum. Clearly, the larger the spacing the lower the sensitivity. Because of various constraints imposed by the need to access the drum surface a minimum distance of 3.5cm was deemed acceptable. This type of accurace is possible because the shift in resonant frequency is approximately 1 MHz per mm rubber thickness. Considering the fact that even the simplest network analyzers can resolve down to less than 1 kHz, one can expect a basic measurement sensitivity of less than 1 micrometer. This computed sensitivity has been proven in experiments with a prior system [15]. As expected, at higher frequencies, the sensitivity should be higher.

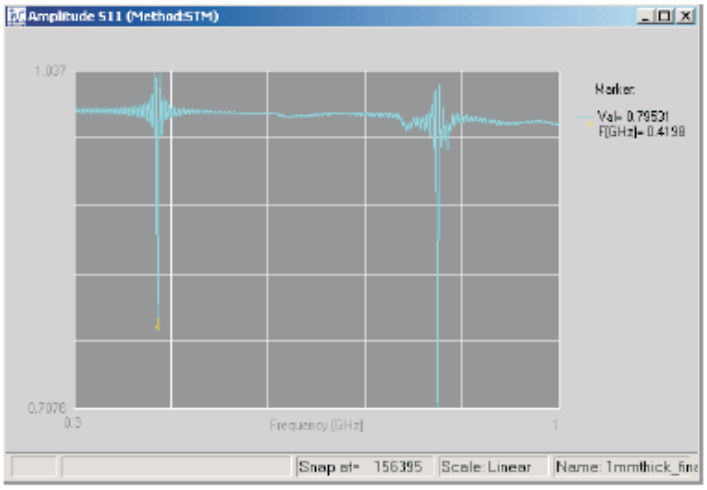

Fig. 9. Screen capture showing the first two resonant frequencies of the resonator in Fig. 8 with a rubber thickness of 1mm and sensor separation of 3.5 cm. The first is at 419.8 MHz, the second at 824.9 MHz.

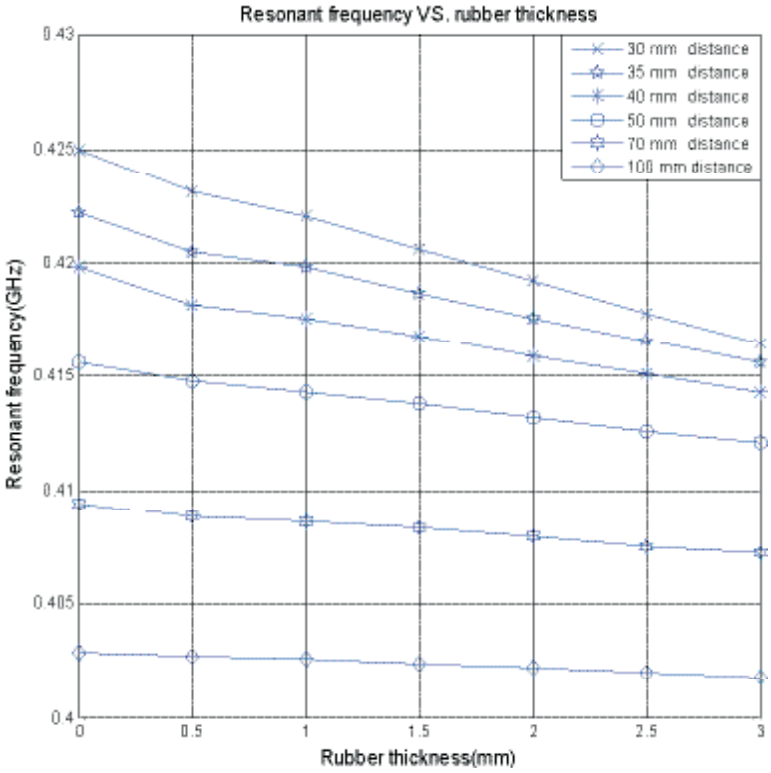

Fig. 10. Lowest resonant frequency versus rubber thickness for various sensor spacings.

6 Conclusion

A numerical model for scanning microwaves microscopy based on the TLM algorithm was discussed and implemented. The results show that the model can be applied to dimensional characterization of structures with different electric permitivities. Analysis of material properties is best done in closed or open resonant structures. To this end we have shown that various structures ranging from fully closed to open resonators can be successfully used and the analysis of these structures is best done with finite element techniques. Sample results show the sensitivity to material properties in lossless and lossy dielectrics. To demonstrate the use of resonant methods to dimensional gauging we have described an open resonator sensor implemented in an industrial application following analysis using FDTD methods. The accuracy of the system is below 1 ?m in spite of the relatively low frequency used.

References

[1] N. Ida, *Microwave NDT*. Kluwer Press, 1992.

[2] M. N. O. Sadiku and C. N. Obiozor, "A comparison of finite difference time-domain (FDTD) and transmission-line modeling (TLM) methods," in *Southeastcon 2000, Proceedings of the IEEE*, 2000, pp. 19–22.

[3] J. Porti and A. Morente, "TLM method and acoustics," *International Journal of numerical modeling*, vol. 14, pp. 171–183, 2001.

[4] P. B. Johns, "A symmetrical condensed node for the tlm method," *IEEE Transaction on Microwave Theory and Techniques*, vol. MTT-35, no. 4, pp. 370–377, 1987.

[5] J. L. Herring, "Developments in the transmission-line modelling method for electromagnetic compatibility studies," Ph.D. dissertation, May 1993.

[6] R. Ciocan and M. Tabib-Azar, "Transient thermography of semiconductors using microwave microscope," *Microscale Thermophysical Engineering*, vol. 3, no. 4, pp. 321–327, 1999.

[7] A. J. Bahr, *Microwave Nondestructive Testing Methods*. Gordon an Breach Science, 1982.

[8] J. S. Wang and N. Ida, "Curvilinear and higher order edge finite elements in electromagnetic field computation," *IEEE Transactions on Magnetics*, vol. 29, no. 2, pp. 1491–1494, Mar. 1993.

[9] M. Fischer, "Microwave stripline sensors for industrial measurement applications," Ph.D. dissertation, Helsinki University of Technology, Radio Laboratory, Nov. 1995, report S 218.

[10] A. J. Kraszewski, "Microwave aquametry needs and perspectives," *IEEE Transactions on Microwave Theory and Techniques*, vol. 39, no. 5, pp. 828–835, May 1991.

[11] E. Nyfors and P. Vainikainen, *Industrial Microwave Sensors*. Norwood, MA: Artech House, 1989.

[12] A. Kjaer, P. Westland, and W. Heath, "On-line sensing of paper machine wet-end properties: dry-line detector," *IEEE Transactions on Control Systems Technology*, vol. 5, no. 6, pp. 571–585, 1997.

[13] R. King and J. Basuel, "Measurement of basis weight and moisture content of composite boards using microwaves," *Forest Products Journal*, vol. 43, no. 9, pp. 15–22, 1993.

[14] R. J. King, K. V. King, and K. Woo, "Microwave moisture measurement of grains," *IEEE Transactions on Instrumentation and Measurements*, vol. IM-41, no. 1, pp. 111–115, 1992.

[15] N. Farahat and N. Ida, "Open stripline resonator for gauging in industrial applications," in *Review of Progress in Applied Computational Electromagnetics-ACES*, Verona, Italy, Apr. 20–24, 2007, pp. 1846–1851.

[16] B. Bhat and S. K. Koul, *Stripline-Like Transmission Lines for Microwave Integrated Circuits*. New York: John Wiley & Sons, 1989.

[17] R. Harrington, *Time-Harmonic Electromagnetic Fields*. New Yotk, NY 10020: McGraw-Hill, 1961.